A Model Predictive Approach to Protect Power Systems against Cascading Blackouts

Chao Zhai, Hehong Zhang, Gaoxi Xiao, and Tso-Chien Pan *

May 13, 2019

Abstract

Large scale blackouts normally go through several sequential phases according to the propagation speed of branch outages and the disruption level of power grids. It is crucial to eliminate the propagation of cascading outages in its infancy. In this paper, a model predictive approach is proposed to protect power grids against cascading blackouts. First of all, the cascading dynamics of power grids is described by the outage model of transmission lines and the DC power flow equation, which allows us to predict the cascading failure path. Then a nonlinear convex optimization formulation is established to terminate the cascading outages by adjusting the injected power on buses. Afterwards two protection schemes are designed according to the optimization formulation: one scheme carries out protective actions to terminate cascading outages once for all, while the other takes protection measures in two consecutive steps. Saddle point dynamics is employed to provide a numerical solution to the proposed optimization problem, and its global convergence is guaranteed in theory. Finally, numerical simulations on IEEE test systems are implemented to validate the proposed approach.

Keywords: Power system protection, model predictive approach, cascading failure, convex optimization, saddle point dynamics.

*Chao Zhai is with School of Automation, China University of Geosciences, Wuhan 430074 China, and with Hubei Key Laboratory of Advanced Control and Intelligent Automation for Complex Systems, Wuhan 430074, China. Chao Zhai, Hehong Zhang and Gaoxi Xiao are with School of Electrical and Electronic Engineering, Nanyang Technological University. Hehong Zhang, Gaoxi Xiao and Tso-Chien Pan are with Institute of Catastrophe Risk Management, Nanyang Technological University, 50 Nanyang Avenue, Singapore 639798. Hehong Zhang, Gaoxi Xiao and Tso-Chien Pan are also with Future Resilient Systems, Singapore-ETH Centre, 1 Create Way, CREATE Tower, Singapore 138602. Corresponding author: Gaoxi Xiao. Email: egxxiao@ntu.edu.sg

1 Introduction

The protection of power grids against cascading blackouts has always been a great challenge to both the power industry and academia due to unexpected contingencies and the evolving nature of power grids [1]. In the last decades, the technologies of phasor measurement, communication and data processing have made great progress, which allows us to detect the real-time state of power systems, transmit the data and generate control signals for emergency control.

The developments of power system protection basically go through three stages [2]. Specifically, the conventional protection of power systems mainly resorts to electro-mechanical protective relay for tripping overloading branches [3]. In spite of high reliability and simplicity in construction, these relays need to be calibrated periodically, and they are unable to determine the direction of a fault with respect to the relay's location. The introduction of computers features the second stage of power system protection as advanced control algorithms can be applied to protect power grids [4, 5]. The third stage is characterized by the utilization of global positioning system (GPS), which enables engineers to synchronize time precisely and obtain the global phase information for the wide-area protection [6]. The availability of global information on power systems allows to establish a systematic approach to cope with catastrophic scenarios in wide-area power networks. Thus, the special protection scheme (SPS) is proposed to mitigate global stresses by separating power systems into several islands and isolating the faulted areas according to predetermined actions [7]. It is demonstrated that the installation of SPSs is economically profitable [8]. Nevertheless, the SPSs are designed for particular power systems suffering from limited unusual stresses (e.g., frequency instability, voltage instability and transient angle instability), which inevitably restricts their compatibility and the universality for contingencies. As a result, some effective protection algorithms are designed to deal with the disruptive contingencies by means of adaptive relaying [9], network of phasor measurements [10] and multi-agent approach [11]. In practice, the signalling latency makes up the critical barrier against the online implementation of protection algorithms [12].

Power system blackouts normally go through five phases: precondition, initiating events, cascade events, final state and restoration [13]. As classified in existing studies [13] and evidenced by previous large blackouts (e.g., [14, 15]), cascade events can be divided into two stages: steady-state progression where the cascades propagate slowly while keeping the balance between the power generation and consumption, and high-speed cascade where the cascades propagate quickly and may end up with the system collapse in a short time. The steady-state progression may give rise to a triggering event (e.g., the tripping of a certain line), which leads to the occurrence of high-speed cascade. In the period of steady-state progression, the cascade overloads are the major incidents, and thus it is feasible to predict the cascading

failure path according to the overloading branches during this period. In this paper, we propose a protection architecture to prevent cascading blackouts by predicting the cascading outages and adjusting the injected power on buses in the period of steady-state progression. Since the DC power flow is a desirable substitute for the AC power flow in high-voltage transmission networks [16, 17], for simplicity, the DC power flow equation is employed to compute the power flow. The main contributions of this work are listed as follows.

1. Propose a disturbance-related real-time protection architecture of power systems by predicting the cascading evolution in the period of steady-state progression.

2. Integrate time delays of faults detection, signal transmission and processing into the protection architecture to achieve reliable protections.

3. Develop two protection schemes to prevent the propagation of cascading outages and succeed in implementing the optimal adjustment of injected power on buses with saddle point dynamics.

The outline of this paper is organized as follows. Section 2 presents the protection architecture of power systems against cascading blackouts. Section 3 provides the optimization formulation of nonrecurring protection scheme and theoretical analysis, followed by the scheme of recurring protection in Section 4. Simulations and validation on IEEE test systems are given in Section 5. Finally, we discuss the extensions of the proposed protection architecture in Section 6 and conclude the paper in Section 7.

2 Protection Architecture

Thanks to phasor measurement units (PMUs), the operating state of modern power grids can be monitored in real time [18, 19]. This enables the wide-area protection and control system (WAPCS) to identify the disturbances or faults as soon as possible [20] and then take remedial actions. In this work, remedial actions mainly refer to the adjustment of injected power on buses (e.g., load shedding, generation ramping/tripping) for protecting power system against blackouts. Specifically, the disturbance-related signals are detected by PMUs and then transmitted to the phasor data concentrator (PDC) [21]. Through the dedicated communication networks (e.g., virtual private network [19]), PDCs send the disturbance-related data to data server and WAPCS, where the disturbances are identified and the cascading process of transmission lines is predicted via the outage model of branches. Finally, the protection architecture produces corrective control signals for local actuators in order to terminate cascading outages. In practice, the local actuators include different relays (e.g., voltage relays and frequency relays) and circuit breakers for

Table 1: Time Delays of Sequential Operations in WAPCS [22, 23].

Sequence	Operation	Time delay
1	Signal detection using PMUs	$\leq$ 150ms
2	Transmission of PMU data	$\leq$ 700ms
3	Generation of control signals	$\approx$ 100ms
4	Transmission of control signals	$\approx$ 10ms
5	Operation of local actuators	$\approx$ 50ms

load shedding, and supplementary controllers and turbine valves for generation control. Time delays of the above sequential operations in WAPCS are summarized in Table 1. The overall time delays from the disturbance detection to the implementation of control command can be roughly estimated. During this period, the power system probably has gone through some cascading failures due to initial contingencies and subsequent branch outages. Thus, proper control and remedial actions should be taken in time by incorporating the above time delays.

In this work, our goal is to develop a protection architecture that integrates wide-area monitoring, prediction and control of power networks so that WAPCS is able to make disturbance-related remedial actions in time to achieve the least power loss during emergency. First of all, we clarify the concept of cascading step in order to describe the evolution of branch outages during cascading blackouts. A cascading step is defined as one topological change (e.g., one branch outage) of power networks due to contingencies, human factors or the overloading of transmission lines during the cascading process. Once the transmission line is overloaded, the timer of circuit breaker will be triggered to count down from the preset time T_p. And the transmission line is tripped when the timer runs out. Thus, the time interval between two consecutive cascading steps basically depends on the preset time of the timer in protective relays [24]. The evolution time of cascading failure is defined as the time duration from the first activation of the timer of circuit breaker to the current time during the cascades. Then the evolution time of cascading failure is $t_c \approx kT_p$ at the k-th cascading step. Remedial/protective actions are taken at a specified cascading step, which ensures that the estimated evolution time of cascades exceeds the total time delay of sequential operations in WAPCS. This work focuses on the evolution of branch outages in the early stage of cascading failure (i.e., the steady-state progression), during which the branch outage basically occurs as a result of branch overloads and running out of preset time in the timer. This enables us to roughly estimate the evolution time of cascading failure based on the cascading steps.

Remark 2.1. *It takes a fixed time delay T_p for the relay to trip the branch once it is overloaded. The timer in the relay starts to count down from the preset time T_p, and the circuit breaker trips the overloaded branch when the timer runs out. The topology of power networks is updated after the overloaded branches are tripped. Then the power flow is recomputed based on the updated topology of power networks. Again the branch is overloaded if the recomputed power flow exceeds the given threshold. In this way, the cascading outage of branches proceeds until the power flow on each branch is less than the threshold. Actually, the proposed protection architecture is also compatible with other types of relays with different temporal operational characteristics, which will introduce the variable time delays of branch outage according to the overloading level. For the tripping delay under different time-inverse characteristics, we can choose the minimum value of T_P (i.e., the minimum reclosing time of circuit breaker) as a fixed time delay to compute the prediction horizon m for the timely implementation of protection actions at the end of prediction horizon.*

To predict the cascading failure path, it is necessary to obtain the cascading dynamics of power networks, which includes the DC power flow equation and the outage model of branches. Consider a power network with n branches and n_b buses, and the initial disturbances δ (e.g., lightening, storm, poor contactor and collapsed vegetation, etc) affect the branch admittance as follows

$$Y_p^1 = Y_p^0 + \delta$$

where $Y_p^0 \in R^n$ refers to the n-dimensional vector of the original branch admittance and Y_p^1 denotes the branch admittance at the first cascading step. For simplicity, the DC power flow equation is employed to compute the power flow on each transmission line.

$$P = A^T diag(Y_p^k) A\theta^k, \quad k \in \mathbb{N} \tag{1}$$

where P denotes the n_b-dimensional vector of injected power on each bus and $A \in R^{n \times n_b}$ refers to the branch-bus incidence matrix [25]. θ^k represents the n_b-dimensional vector of voltage angle on each bus at the k-th cascading step. In addition, the operation $diag(x)$ obtains a square diagonal matrix with the elements of vector x on the main diagonal. The solution to Equation (1) is expressed as

$$\theta^k = (A^T diag(Y_p^k) A)^{-1^*} P$$

where the operator -1^* is used to compute the inverse of a square matrix, as defined in [26] (see Subsection 8.1 in Appendix). Thus, the vector of power flow on branches is $diag(Y_p^k)A(A^T diag(Y_p^k)A)^{-1^*}P$. According to Lemma 3.2 in [26] (see Subsection 8.2 in Appendix), the power flow from Bus i to Bus j

at the k-th cascading step is given by

$$P_{ij}^k = e_i^T A^T diag(Y_p^k) A e_j (e_i - e_j)^T (A^T diag(Y_p^k) A)^{-1^*} P, \tag{2}$$

with $i, j \in I_{n_b} = \{1, 2, ..., n_b\}$, where e_i represents the n_b dimensional unit vector with the i-th element being 1 and other elements being 0. The evolution of branch admittance (i.e., the outage model of branches) is described by the following formula

$$Y_p^{k+1} = \begin{cases} Y_p^k + \delta, & k = 0; \\ \mathscr{G}(P_{ij}^k) \circ Y_p^k, & k \geq 1. \end{cases} \tag{3}$$

where the operator $\circ$ represents the Hadamard product and $\mathscr{G}(P_{ij}^k)$ is given by

$$\mathscr{G}(P_{ij}^k) = (g(P_{i_1 j_1}^k, c_{i_1 j_1}), g(P_{i_2 j_2}^k, c_{i_2 j_2}), ..., g(P_{i_n j_n}^k, c_{i_n j_n}))^T.$$

And therein is the approximation function [26]

$$g(P_{ij}^k, c_{ij}) = \begin{cases} 0, & |P_{ij}^k| \geq \sqrt{c_{ij}^2 + \frac{\pi}{2\sigma}}; \\ 1, & |P_{ij}^k| \leq \sqrt{c_{ij}^2 - \frac{\pi}{2\sigma}}; \\ \frac{1 - \sin\sigma\left[(P_{ij}^k)^2 - c_{ij}^2\right]}{2}, & \text{otherwise.} \end{cases}$$

where c_{ij} denotes the threshold of power flow on the transmission line connecting Bus i to Bus j. The approximation function is introduced to describe the change of branch admittance when the power flow exceeds the threshold and the transmission line is tripped by the circuit breaker. It gets close to the step function that reflects the real system characteristic of branch outage when the parameter σ increases. Moreover, it is differentiable with respect to P_{ij}^k, which ensures the feasibility of optimal adjustment of injected power on buses in protection schemes.

Essentially, the protection architecture is composed of three building blocks including contingency identification, prediction of cascading failure and protection schemes (see Fig. 1). It is in line with the typical architecture of wide-area monitoring, protection and control system [19]. The disturbance is identified by WAPCS [20], then it triggers the evolution of cascading dynamics, which is composed of the DC power flow equation (1) and the outage model of branches (3). When the power network is split into isolated subnetworks, the generator bus connected to the largest generating station is selected as the new slack bus in the subnetwork. And thus the power variation of slack bus accounts for a small percentage of its generating capacity. Then the DC power flow is solved for each subnetwork to redistribute the power flow. Significantly, the cascading dynamics allows us to preplan remedial actions by taking into account the time delays of sequential operations and solving the optimization problem in protection schemes.

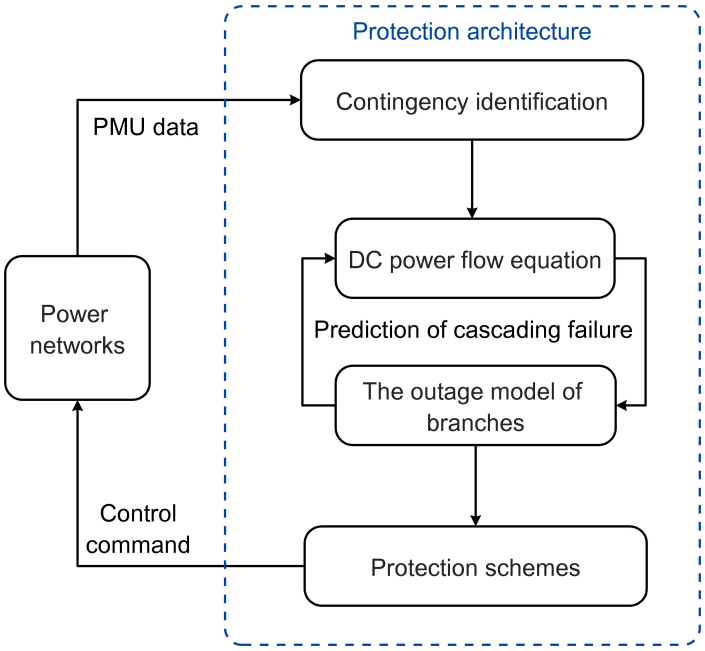

Figure 1: Protection architecture of power systems.

After power blackouts are prevented by implementing the control commands from protection schemes, the protection architecture starts the detection and identification of disturbances once again. Thus, the key task is to design the effective protection schemes to terminate the propagation of cascading outages. The current practices for power system emergency largely resort to the predetermined protection actions in the SPS. Compared to the SPS, our approach requires the real-time computation of mitigating actions for the specific power system state. It can effectively reduce the cost of power system protection and increase the flexibility of power grids to deal with the diverse emergencies.

Remark 2.2. *Mathematically, the cascading failure process of power grids can be regarded as a series of operations/transformations on a mathematical model (i.e., the outage model of branches) that characterizes the redistribution of power flow and protective relays in power systems. And protection schemes ensure that the cascading failure process converges towards a desired fixed point, which stabilizes power grids with the least cost.*

In the subsequent two sections, we propose two different protection schemes (i.e., nonrecurring protection scheme and recurring protection scheme).

3 Nonrecurring Protection Scheme

This section presents the first scheme, i.e. Nonrecurring Protection Scheme (NPS). NPS implies that protective actions are taken only once at a given cascading step. Due to time delays in WAPCS, we will only be able to carry out the optimal adjustment of injected power on buses against the propagation of cascading failures at the m-th cascading step. And thus the evolution time of cascading failure is $t_c \approx mT_p$, which should be larger than the total time delays in WAPCS so that protective actions are available at the m-th cascading step. Specifically, the value of prediction horizon m should satisfy $m \cdot T_p > T_{delay} + T_{detection} + T_{run} + T_{actuation}$ with time delay of data transmission T_{delay}, the detection time of disruptive disturbances $T_{detection}$, the runtime of numerical algorithm T_{run}, and the actuation time of relays $T_{actuation}$. In this way, the protection architecture is ready to take protective actions (i.e., optimal adjustment of injected power on buses) when the cascading failure reaches the m-th cascading step. The optimization problem can be formulated as

$$\begin{aligned} &\min_{P} J(P,W) \\ s.t.\ \ &Y_p^m = \mathscr{G}(P_{ij}^{m-1}) \circ \mathscr{G}(P_{ij}^{m-2}) \circ \cdots \circ \mathscr{G}(P_{ij}^{1}) \circ Y_p^1 \\ &P_{ij}^m = e_i^T A^T diag(Y_p^m) A e_j (e_i - e_j)^T (A^T diag(Y_p^m) A)^{-1^*} P \\ &(P_{ij}^m)^2 \le c_{ij}^2, \quad (i,j) \in \mathscr{E} \\ &\underline{P}_i \le P_i \le \bar{P}_i, \quad i \in I_{n_b} \end{aligned} \tag{4}$$

where the objective function $J(P,W)$ is given by

$$J(P,W) = \|W \circ (P - P^0)\|^2 \tag{5}$$

P^0 represents the vector of original injected power on each bus, and $P = (P_1, P_2, ...P_{n_b})^T$ refers to the injected power vector after the adjustment. $\underline{P}_i$ and $\bar{P}_i$ denote the lower and upper bounds of injected power on Bus i, respectively. The weight vector $W = (W_1, W_2, ..., W_{n_b})^T$ characterizes the bus significance in power systems, and P_{ij}^m denotes the power flow on the branch connecting Bus i and Bus j at the m-th cascading step.

The cost function of Problem (4) characterizes the mismatch of injected power on each bus between the original distribution of load and power generation and the reassigned one from the optimization algorithm. The first term in the constraint conditions predicts the cascading process of power grids before taking remedial measures. The second term calculates the power flow on each branch at the m-th cascading step, and the third one imposes the restriction on the upper bound of power flow on each branch. The final term stipulates the adjustment range of injected power on each bus. Moreover, it can be observed that Optimization Problem (4) is convex.

Remark 3.1. *T_P largely depends on the parameter setting of protective relays (normally larger than $0.3s$). In addition, the parameters T_{delay}, $T_{detection}$, T_{run} and $T_{actuation}$ can be roughly estimated for the actual power grid and the WAPCS (see Table 1). Thus, the prediction horizon m can be chosen by*

$$m = \left\lceil \frac{T_{delay} + T_{detection} + T_{run} + T_{actuation}}{T_p} \right\rceil,$$

where the symbol $\lceil x \rceil$ gives the least integer that is greater than the real number x.

Proposition 3.1. *Optimization Problem (4) is convex.*

Proof. The cost function $J(P,W)$ and the constraint function $(P_{ij}^m)^2 - c_{ij}^2$ are convex, and P_{ij}^m is affine with respect to P. Thus, (4) is a convex optimization problem. □

Then we present the necessary and sufficient condition for the optimal solution to Optimization Problem (4).

Proposition 3.2. *Suppose Slater's condition holds (nonempty feasible region) for Convex Optimization Problem (4). Then P^* is the optimal solution if and only if there exist Lagrangian multipliers λ_{ij}^*, $\bar{\tau}_i^*$ and $\underline{\tau}_i^*$ satisfying the KKT conditions:*

$$\nabla J(P^*,W) + \sum_{i=1}^{n_b}\sum_{j=1}^{n_b} \lambda_{ij}^* \nabla \left[(P_{ij}^{m*})^2 - c_{ij}^2\right] + \sum_{i=1}^{n_b} (\bar{\tau}_i^* - \underline{\tau}_i^*) e_i = \mathbf{0}$$

and

$$\begin{aligned}
&(P_{ij}^{m*})^2 \le c_{ij}^2 \\
&P_{ij}^{m*} = e_i^T A^T diag(Y_p^m) A e_j (e_i - e_j)^T (A^T diag(Y_p^m) A)^{-1^*} P^* \\
&\underline{P}_i \le P_i^* \le \bar{P}_i \\
&\lambda_{ij}^* [(P_{ij}^{m*})^2 - c_{ij}^2] = 0 \\
&\bar{\tau}_i^* (P_i^* - \bar{P}_i) = 0 \\
&\underline{\tau}_i^* (\underline{P}_i - P_i^*) = 0
\end{aligned}$$

Proof. The result directly follows from Theorems 3.25-3.27 in [27]. □

Actually, many numerical methods are available to solve Convex Optimization Problem (4). Here, Saddle Point Dynamics is employed due to its great success in designing distributed network control protocols [28, 29], which helps to enhance the resilience of power systems. Design the following Lagrangian function

$$L(P,\lambda,\tau) = J(P,W) + \sum_{(i,j)\in\mathscr{E}} \lambda_{ij} \left[(P_{ij}^m)^2 - c_{ij}^2\right] + \sum_{i=1}^{n_b} \bar{\tau}_i (P_i - \bar{P}_i) + \sum_{i=1}^{n_b} \underline{\tau}_i (\underline{P}_i - P_i)$$

where (i,j) is an element of set $\mathscr{E}$ if Bus i and Bus j are connected in power networks. According to Saddle Point Theorem in [27], the optimal solution P^* to Optimization Problem (4) satisfies the KKT condition in Proposition 3.2 with Lagrangian multipliers λ^* and τ^* if and only if (P^*,λ^*,τ^*) is a saddle point of the Lagrangian function $L(P,\lambda,\tau)$. Next, we present the saddle point dynamics to search for the saddle point of Lagrangian function $L(P,\lambda,\tau)$ [30].

$$\begin{aligned}
\dot{P} &= -\nabla_P L(P,\lambda,\tau) \\
&= -2W\circ(P-P^0) - 2\sum_{(i,j)\in\mathscr{E}} \lambda_{ij} P_{ij}^m R_{ij}^m - (\bar{\tau}-\underline{\tau}) \\
\dot{\lambda}_{ij} &= [\nabla_{\lambda_{ij}} L(P,\lambda,\tau)]^+_{\lambda_{ij}} = [(P_{ij}^m)^2 - c_{ij}^2]^+_{\lambda_{ij}} \\
\dot{\bar{\tau}}_i &= [\nabla_{\bar{\tau}_i} L(P,\lambda,\tau)]^+_{\bar{\tau}_i} = [P_i - \bar{P}_i]^+_{\bar{\tau}_i} \\
\dot{\underline{\tau}}_i &= [\nabla_{\underline{\tau}_i} L(P,\lambda,\tau)]^+_{\underline{\tau}_i} = [\underline{P}_i - P_i]^+_{\underline{\tau}_i}
\end{aligned} \tag{6}$$

where

$$R_{ij}^m = e_i^T A^T diag(Y_p^m) A e_j \cdot \left[(A^T diag(Y_p^m)A)^{-1^*}\right]^T (e_i - e_j)$$

and the operator $[\,]^+$ is defined as

$$[x]^+_y = \begin{cases} x, & y>0; \\ \max\{x,0\}, & y=0. \end{cases} \tag{7}$$

Significantly, it is guaranteed in theory that Saddle Point Dynamics (6) approaches the optimal solution of Optimization Problem (4) as time goes to infinity.

Proposition 3.3. *Saddle Point Dynamics (6) globally asymptotically converges to the optimal solution to Optimization Problem (4).*

Proof. See Subsection 8.3 in Appendix. □

Finally, we summarize the Nonrecurring Protection Scheme in Table 2. First of all, we set the number of cascading steps m and estimate the evolution time of cascading failure $t_c \approx mT_p$ for protective actions. NPS detects electrical signals of power network in real time with the aid of PMUs and then estimates the current branch admittance vector $Y_p(t)$ [20]. This allows WAPCS to locate the disturbed branches by comparing the current branch admittance vector $Y_p(t)$ with the original one Y_p^0. Then NPS computes the admittance changes on the branches to identify the disturbance δ. The above disturbance initiates the cascading process to predict the state of power grids at the m-th cascading step, which enables us to solve Saddle Point Dynamics (6) and work out remedial actions. When the cascading failure evolves to the m-th step, WAPCS will take the remedial actions of adjusting injected power on buses. Finally, NPS computes the power flow on each branch to validate the remedial actions.

Table 2: Nonrecurring Protection Scheme.

1: Detect electrical signals using PMUs
2: Estimate branch admittance vector $Y_p(t)$
3: **if** $(Y_p(t) \neq Y_p^0)$
4: Identify the disturbance $\delta = Y_p(t) - Y_p^0$
5: Initiate cascading dynamics with (2) and (3)
6: Save system state at the m-th cascading step
7: Solve Saddle Point Dynamics (6)
8: **if** $(k = m)$
9: Take protective actions with solutions to (6)
10: **end if**
11: Compute the power flow on each branch
12: **else**
13: Go back to Step 1
14: **end if**

4 Recurring Protection Scheme

In this section, we propose the second scheme, *i.e*. Recurring Protection Scheme (RPS), with which WAPCS takes remedial actions and implements the corrective control by adjusting the injected power on buses at two consecutive cascading steps (*i.e*., $m-1$ and m). Compared with NPS, more control variables are available in RPS to optimize the objective function. Essentially, RPS increases the flexibility of preventing cascading outages. Theoretically, the optimization formulation of RPS can be presented as

$$\begin{aligned}
&\min_{P^k} \ \mathscr{C}(P^{m-1}, P^m, W) \\
s.t. \ &P_{ij}^k = e_i^T A^T diag(Y_p^k) A e_j (e_i - e_j)^T (A^T diag(Y_p^k) A)^{-1^*} \tilde{P}^k \\
&Y_p^{k+1} = \mathscr{G}(P_{ij}^k) \circ Y_p^k \\
&(P_{ij}^m)^2 \le c_{ij}^2, \quad (i,j) \in \mathscr{E} \\
&\underline{P}_i \le \tilde{P}_i^k \le \bar{P}_i, \quad i \in I_{n_b}, \quad k \in \{m-1, m\}
\end{aligned} \tag{8}$$

where

$$\mathscr{C}(P^{m-1}, P^m, W) = \|W \circ (P^{m-1} - P^0)\|^2 + \|W \circ (P^m - P^0)\|^2$$

and

$$\tilde{P}^k = \begin{cases} P^0, & k \le m-2; \\ P^k, & \text{otherwise.} \end{cases}$$

Remark 4.1. *It is assumed that the fluctuation of P^k is negligible prior to load shedding and generator ramping/tripping. Thus, the value of P^k keeps constant (i.e., P^0) in the optimization formulations (4) and (8) before implementing protection schemes. Actually, the above optimization formulations are applied to the case with the time-varying values of P^k when the dynamics of P^k ($1 \le k \le m-1$) is available.*

Proposition 4.1. *Solutions to Optimization Problem (8) do not underperform those to the Convex Optimization Problem (4) in terms of minimizing the changes of injected power on buses.*

Proof. Let $P^{k*}, k \in \{m-1, m\}$ denote the solution to Optimization Problem (8), and P^* represents the solution to Convex Optimization Problem (4). Then it follows from

$$\|W \circ (P^{m*} - P^0)\|^2 \le \mathscr{C}(P^{(m-1)*}, P^{m*}, W) \le \mathscr{C}(P^0, P^*, W) = \|W \circ (P^* - P^0)\|^2$$

that

$$\|W \circ (P^{m*} - P^0)\|^2 \le \|W \circ (P^* - P^0)\|^2,$$

which completes the proof. □

Actually, it is difficult to obtain the optimal solution to Optimization Problem (8) due to its non-convexity. The linearized method can be applied to approximate the non-convex constraint for achieving the global optima. To simplify mathematical expressions, we define

$$\mathscr{F}(Y_p^k) = e_i^T A^T diag(Y_p^k) A e_j (e_i - e_j)^T (A^T diag(Y_p^k) A)^{-1^*}$$

Then we obtain $P_{ij}^k = \mathscr{F}(Y_p^k)\tilde{P}^k$ and

$$\begin{aligned} P_{ij}^m &= \mathscr{F}(Y_p^m)P^m \\ &= \mathscr{F}\left[\mathscr{G}(P_{ij}^{m-1}) \circ Y_p^{m-1}\right] P^m \\ &= \mathscr{F}\left[\mathscr{G}(\mathscr{F}(Y_p^{m-1})P^{m-1}) \circ Y_p^{m-1}\right] P^m \end{aligned}$$

The gradient of P_{ij}^m with respect to $[P^{m-1}, P^m]$ is given by

$$\nabla P_{ij}^m = \begin{pmatrix} \nabla_{Y_p^m}\left[\mathscr{F}(Y_p^m)P^m\right]^T \left[\mathscr{G}'(\mathscr{F}(Y_p^{m-1})P^{m-1}) \circ Y_p^{m-1}\right] \\ \cdot \mathscr{F}(Y_p^{m-1})^T \\ \mathscr{F}\left[\mathscr{G}(\mathscr{F}(Y_p^{m-1})P^{m-1}) \circ Y_p^{m-1}\right]^T \end{pmatrix}$$

Therefore, $P_{ij}^m = \mathscr{F}(Y_p^m)P^m$ can be approximated by the following linear equation in the neighborhood of $[P^0, P^0]$.

$$\begin{aligned} \hat{P}_{ij}^m|_{[P^0,P^0]} = {} & \nabla_{Y_p^m}\left[\mathscr{F}(Y_p^m|_{P^0})P^0\right]^T \left[\mathscr{G}'(\mathscr{F}(Y_p^{m-1})P^0) \circ Y_p^{m-1}\right] \mathscr{F}(Y_p^{m-1})(P^{m-1} - P^0) \\ & + \mathscr{F}\left[\mathscr{G}(\mathscr{F}(Y_p^{m-1})P^0) \circ Y_p^{m-1}\right] P^m \end{aligned} \tag{9}$$

where $Y_p^m|_{P^0} = \mathscr{G}(\mathscr{F}(Y_p^{m-1})P^0) \circ Y_p^{m-1}$. In this way, Optimization Problem (8) can be approximated by the following problem.

$$\begin{aligned} & \min_{P^k} \ \mathscr{C}(P^{m-1}, P^m, W) \\ s.t. \ & \hat{P}_{ij}^m = \nabla_{Y_p^m}\left[\mathscr{F}(Y_p^m|_{P^0})P^0\right]^T \left[\mathscr{G}'(\mathscr{F}(Y_p^{m-1})P^0) \circ Y_p^{m-1}\right] \mathscr{F}(Y_p^{m-1})(P^{m-1} - P^0) \\ & \quad + \mathscr{F}\left[\mathscr{G}(\mathscr{F}(Y_p^{m-1})P^0) \circ Y_p^{m-1}\right] P^m \\ & (\hat{P}_{ij}^m)^2 \le c_{ij}^2, \quad (i,j) \in \mathscr{E} \\ & \underline{P}_i \le P_i^k \le \bar{P}_i, \quad i \in I_{n_b}, \quad k \in \{m-1, m\} \end{aligned} \tag{10}$$

Proposition 4.2. *Optimization Problem (10) is convex.*

Proof. The objective function $\mathscr{C}(P^{m-1}, P^m, W)$ is convex, and $\hat{P}_{ij}^m$ is an affine function of variables P^{m-1} and P^m. Also, $(\hat{P}_{ij}^m)^2 - c_{ij}^2$ is convex. This indicates that Optimization Problem (10) is convex. □

Next, we discuss the numerical solution to Optimization Problem (10). Design the Lagrangian function for Optimization Problem (10) as follows

$$\begin{aligned} L(P^m, P^{m-1}, \lambda, \tau) = \mathscr{C}(P^{m-1}, P^m, W) \\ + \sum_{i=1}^{n_b} \left[\bar{\tau}_i^m (P_i^m - \bar{P}_i) + \bar{\tau}_i^{m-1} (P_i^{m-1} - \bar{P}_i) \right] \\ + \sum_{i=1}^{n_b} \left[\underline{\tau}_i^m (\underline{P}_i - P_i^m) + \underline{\tau}_i^{m-1} (\underline{P}_i - P_i^{m-1}) \right] \\ + \sum_{(i,j)\in\mathscr{E}} \lambda_{ij} \left[(\hat{P}_{ij}^m)^2 - c_{ij}^2 \right] \end{aligned}$$

Saddle point dynamics to search for the saddle point of Lagrangian function $L(P^m, P^{m-1}, \lambda, \tau)$ is given by

$$\begin{aligned} \dot{P^k} &= -\nabla_{P^k} L(P^m, P^{m-1}\lambda, \tau) \\ &= -2W \circ (P^k - P^0) - 2 \sum_{(i,j)\in\mathscr{E}} \lambda_{ij} \hat{P}_{ij}^m R_{ij}^k - (\bar{\tau}^k - \underline{\tau}^k) \\ \dot{\lambda}_{ij} &= [\nabla_{\lambda_{ij}} L(P, \lambda, \tau)]_{\lambda_{ij}}^+ = [(\hat{P}_{ij}^m)^2 - c_{ij}^2]_{\lambda_{ij}}^+ \\ \dot{\bar{\tau}}_i^k &= [\nabla_{\bar{\tau}_i^k} L(P, \lambda, \tau)]_{\bar{\tau}_i^k}^+ = [P_i^k - \bar{P}_i]_{\bar{\tau}_i^k}^+ \\ \dot{\underline{\tau}}_i^k &= [\nabla_{\underline{\tau}_i^k} L(P, \lambda, \tau)]_{\underline{\tau}_i^k}^+ = [\underline{P}_i - P_i^k]_{\underline{\tau}_i^k}^+ \end{aligned} \tag{11}$$

where $k \in \{m-1, m\}$ and

$$R_{ij}^k = \begin{cases} \nabla_{Y_p^m} \left[\mathscr{F}(Y_p^m|_{P^0}) P^0 \right]^T \left[\mathscr{G}'(\mathscr{F}(Y_p^{m-1}) P^0) \circ Y_p^{m-1} \right] \\ \cdot \mathscr{F}(Y_p^{m-1})^T, \quad k = m-1 \\ \mathscr{F} \left[\mathscr{G}(\mathscr{F}(Y_p^{m-1}) P^0) \circ Y_p^{m-1} \right]^T, \quad k = m \end{cases}$$

and the operator $[\,]^+$ is defined in equation (7).

Remark 4.2. *The solution to Optimization Problem (10) merely guarantees $|\hat{P}_{ij}^m| \le c_{ij}$ instead of $|P_{ij}^m| \le c_{ij}, \forall (i,j) \in \mathscr{E}$. Therefore, it is necessary to check whether the constraints $|P_{ij}^m| \le c_{ij}, \forall (i,j) \in \mathscr{E}$ hold after adjusting the injected power on buses at the $(m-1)$-th step and the m-th step according to the solution to (10). The solution to (6) can be adopted as a remedy if there exists $(i,j) \in \mathscr{E}$ such that $|P_{ij}^m| > c_{ij}$.*

Remark 4.3. *For the RPS, only two consecutive steps are taken into consideration for protective actions, because protective actions on more cascading steps will greatly increase the computational complexity of the optimization problem and thus require more time for its numerical solutions. This may delay the real-time implementation of protection schemes.*

Table 3: Recurring Protection Scheme.

1: Detect electrical signals using PMUs
2: Estimate branch admittance vector $Y_p(t)$
3: **if** $(Y_p(t) \neq Y_p^0)$
4: Identify the disturbance $\delta = Y_p(t) - Y_p^0$
5: Initiate cascading dynamics with (2) and (3)
6: Get system states at the $(m-1)$-th cascading step
7: Solve Saddle Point Dynamics (11)
8: Calculate $P_{ij}^m, \forall (i,j) \in \mathscr{E}$ with solutions to (11)
9: **if** $(\lvert P_{ij}^m \rvert \leq c_{ij}, \forall (i,j) \in \mathscr{E})$
10: Solution to (11) $\Rightarrow P_{sl}$
11: **else**
12: Solution to (6) $\Rightarrow P_{sl}$
13: **end if**
14: **if** $(k \in \{m-1, m\})$
15: Take protective actions according to P_{sl}
16: **end if**
17: Compute the power flow on each branch
18: **else**
19: Go back to Step 1
20: **end if**

In theory, we can guarantee that Saddle Point Dynamics (11) achieves the asymptotic convergence of global optimal solution to Optimization Problem (10).

Proposition 4.3. *Saddle Point Dynamics (11) globally asymptotically converges to the optimal solution to Convex Optimization Problem (10).*

Proof. The proof follows by the same argument as that of Proposition 3.3, and is thus omitted. □

Table 3 presents the procedure of RPS, which resembles NPS except for controllable cascading steps and Saddle Point Dynamics (11). Compared with NPS, RPS adjusts the injected power on buses to prevent cascading outages at two consecutive cascading steps ($k \in \{m-1, m\}$). If RPS fails to prevent

further cascading outages through the model validation of two consecutive protective actions, the one-off protection from the solution to (6) takes effect as a remedy. In practice, NPS and RPS are two independent mechanisms that cannot be executed subsequently in one potential cascade. In other words, if RPS is executed, NPS will not be executed, and vice versa. Essentially, NPS can be regarded as a special case of RPS by specifying protection actions at a given cascading step. Normally, more branches can be protected if the prediction horizon m is shorter. This implies that NPS with a shorter prediction horizon probably outperforms RPS with a relative long prediction horizon. In addition, NPS and RPS are designed based on the steady-state assumption. If the assumption fails to hold, the SPS is initiated as a remedy to protect power grids against blackouts.

Remark 4.4. *Different types of relays introduce variable line tripping delays based on the severity of overloading. The outage model of branches can be improved to reflect the temporal operational characteristics of relays, and the variable time delays of line tripping can be roughly estimated based on the overloading level. Thus, this does not affect the applicability and performance of protection schemes (i.e., NPS and RPS).*

Remark 4.5. *NPS and RPS allow for both load shedding and generation ramping/tripping while implementing protection actions against cascading blackouts. The generation ramping/tripping can be achieved by adjusting the injected power on generator buses, and load shedding can be achieved by adjusting the injected power on load buses. Moreover, the generator is tripped when the injected power on the generator bus is adjusted to its lower bound. In practice, the generation ramping/tripping shall be applied first before any load shedding is called. Actually, the proposed optimization formulation is able to allow for the order of protection actions (i.e., generation ramping/tripping and load shedding). Specifically, the optimization problems (4) and (10) can be solved by specifying the constant load and the variable power generation on buses, which can be achieved by adjusting the lower and upper bounds of P_i in (4) and P_i^k in (10). If the solutions to the above optimization problems are available, the generation ramping/tripping can be applied to prevent the cascading failure without load shedding. If there are no feasible solutions, the original optimization problems (4) and (10) should be solved to obtain the optimal injected power on both load buses and generator buses. In this way, the generation ramping/tripping can be applied first, immediately followed by load shedding in order to prevent the cascades.*

5 Numerical Simulations

In this section, we validate and compare two protection schemes (i.e., NPS and RPS) on IEEE test Systems. Two flow charts are presented to illustrate the simulations of NPS and RPS, respectively (see

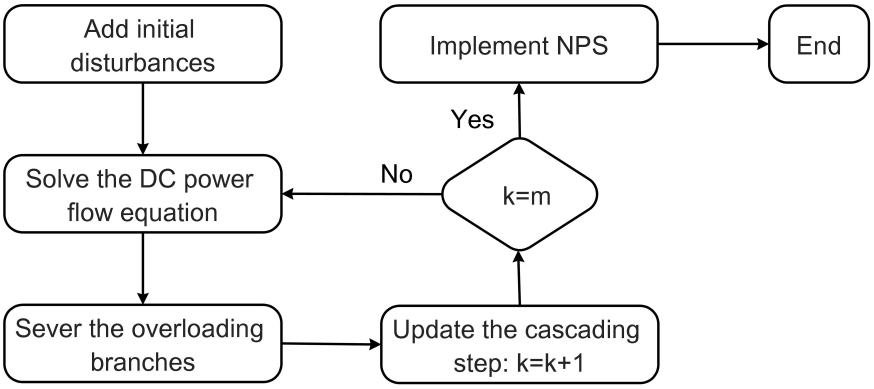

(a) Implementation of NPS

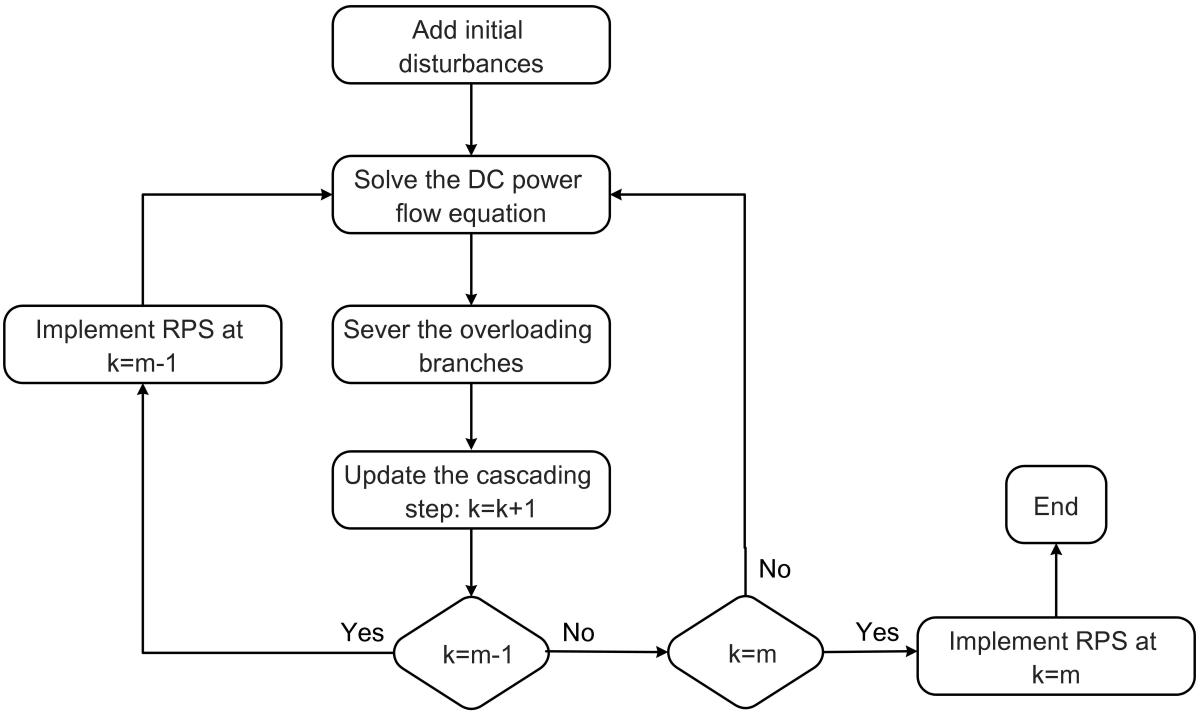

(b) Implementation of RPS

Figure 2: Flow chart of simulations for two protection schemes (a) NPS and (b) RPS.

Fig. 2). Specifically, the disturbance is added on the selected branch with the initial cascading step $k = 0$. Then the power flow on each branch is computed by solving the DC power flow equation. The overloading branch will be tripped once its timer runs out of the preset time in the outage model of branches. When the cascading process arrives at the specified steps (i.e., $k = m$ for NPS, $k = m - 1$ and $k = m$ for RPS), the protection schemes (NPS or RPS) are initiated to prevent further cascading outage of power grids.

5.1 Parameter Setting

The parameter setting for both NPS and RPS is given in detail as follows. For simplicity, we set $W = (1, 1, ..., 1)^T$ to ensure that all buses are equally treated in protection schemes. Per unit values are adopted with the base value of power 100MV in the simulations. The preset time of the timer is $T_p = 1$s in protective relays. The minimum injected power on each bus is equal to the negative value of its total load, and the maximum injected power is provided by the generator connected to this bus. For load buses, their maximum injected power is 0. Consequently, for load buses, we set $\bar{P}_i = 0$ and $\underline{P}_i$ is the total injected power. For generator buses, $\bar{P}_i$ is the total power from the generator, while $\underline{P}_i$ is the injected power from the load. The threshold of power flow on each branch is 1 pu with $\sigma = 10^3$ in the approximation function. In addition, Euler method is employed to implement the numerical algorithms (6) and (11) with the step size 0.01.

5.2 Validation and Comparison

If the branch connecting Bus 9 and Bus 11 (*i.e.*, Branch 10) is tripped as the initial disturbance of IEEE 57 Bus Systems, the cascading process comes to an end after 6 cascading steps ($t_c \approx 6$s) without protection schemes. Branch 10 is selected to add the initial contingency because it can result in the relatively severe cascading failure. Actually, other branches can also be chosen to trigger the cascades. Figure 3 shows the final configuration of IEEE 57 Bus Systems after suffering from the above disturbance. Red balls represent the generator buses, while green ones denote the load buses. Bus ID is also marked on each ball, and the cyan links refer to branches in power systems. The power system ends up with 43 connected branches (5 branches with the power flow) and the total power flow is 1.004pu. Notably, the power network is separated into 5 islands encircled with the dashed curves and 13 isolated buses. Two islands survive due to the power supply from their respective generator buses (Bus 6 and Bus 12), while other three islands without generator buses go through blackouts. In Fig. 3, two islands subject to blackouts include a lot of load buses, which implies that the initial contingency results in the large

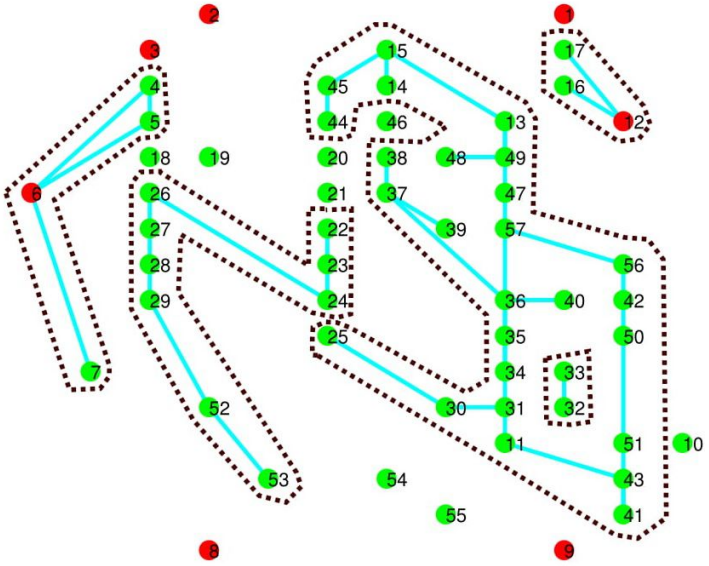

Figure 3: Final configuration of the IEEE 57 Bus System without protection schemes.

disruptions of power grids in terms of power supply. Thus, it is crucial to initiate the real-time protection schemes during the emergency in order to terminate the cascading blackout.

In contrast, Figure 4 presents the final configuration of IEEE 57 Bus Systems with protection schemes (NPS or RPS) after adding the same disturbance (i.e., tripping Branch 10) as that in Figure 3. It is observed that the power system is well protected since most branches in the network are in a good state of transmitting power flow among buses. The power network is decomposed into 3 islands and 9 isolated buses with 53 connected branches. Two islands are composed of generator buses (Bus 6, Bus 9 and Bus 12), while blackouts occur on the island that only includes load buses (Bus 32 and Bus 33). Thanks to NPS and RPS, a lot of load buses can still obtain the power supply in spite of the separation of the whole power network. This indicates the effectiveness of protection schemes in protecting power grids against blackouts. Specifically, for NPS, the cascading process stops after implementing the optimal adjustment of injected power on buses at the 4th cascading step ($t_c \approx 4$s), and the system remains unchanged since then, with the total power flow of 9.156pu. Moreover, the objective function is minimized with the value of 0.1068. Let $\Delta P_k = P^k - P^0$, $k \in \{3,4\}$ denote the vector of load change on each bus at the k-th cascading step. Figure 5 shows the distribution of changes of injected power on each bus according to NPS. There are no negative values for the changes of injected power on buses, which implies the absence of generator tripping during power systems protection. In Fig. 5, the largest change of injected power occurs on Bus 51 using NPS, and its variation magnitude exceeds 0.1pu.

By adjusting injected power on buses at the 3rd and the 4th cascading steps, RPS succeeds in pre-

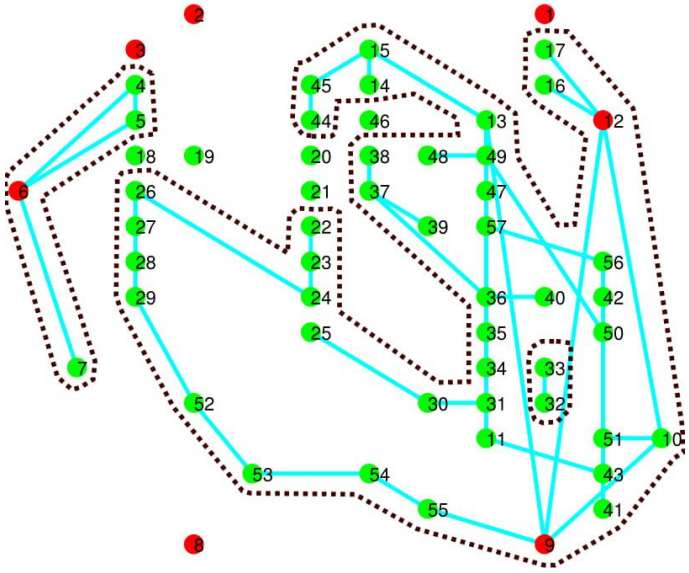

Figure 4: Final configuration of the IEEE 57 Bus System with protection schemes (NPS or RPS).

venting the cascading outage at the 4th cascading step ($t_c \approx 4$s). The total power flow is 12.496pu, and the value of objective function is 0.0979 in the end, less than 0.1068 in NPS. This demonstrates the better performance of RPS to maintain the power transmission and prevent cascading outages in spite of high computational cost. Figure 6 presents the distribution of changes of injected power on each bus using RPS. The green bars denote the changes of injected power on buses at the 3rd cascading step ($t_c \approx 3$s), while the blue ones refer to those at the 4th cascading step ($t_c \approx 4$s). Note that the negative values at Bus 3 and Bus 12 indicate the decrease of power supply to these generator buses. In Fig. 6, four buses (i.e., Bus 1, Bus 3, Bus 8 and Bus 12) adjust their respective injected power at the 3rd and 4th cascading steps, while other buses only adjust the injected power at the 4th cascading step. Moreover, the total change of injected power on Bus 8 is the largest of all buses and it exceeds 0.2 pu.

To compare NPS and RPS in depth, we consider the effect of different operating points (i.e., prediction horizon m) on the performance of two schemes. As we can observe in Fig. 7, NPS and RPS lead to the same performance in terms of N_{cb} and N_{ab} (as green balls and red balls are all overlapping) for each different prediction horizon m. In terms of the total power flow P_t, RPS performs better than NPS in the power transmission because it can contribute to having more total power flow when $m < 5$. As for the changes of injected power on buses P_m, RPS can protect power grids with a lower cost (i.e., fewer changes of injected power on buses) when $m \leq 5$. This partially validates theoretical results in Proposition 4.1. It is worth pointing out that NPS and RPS perform the same for all four indexes when

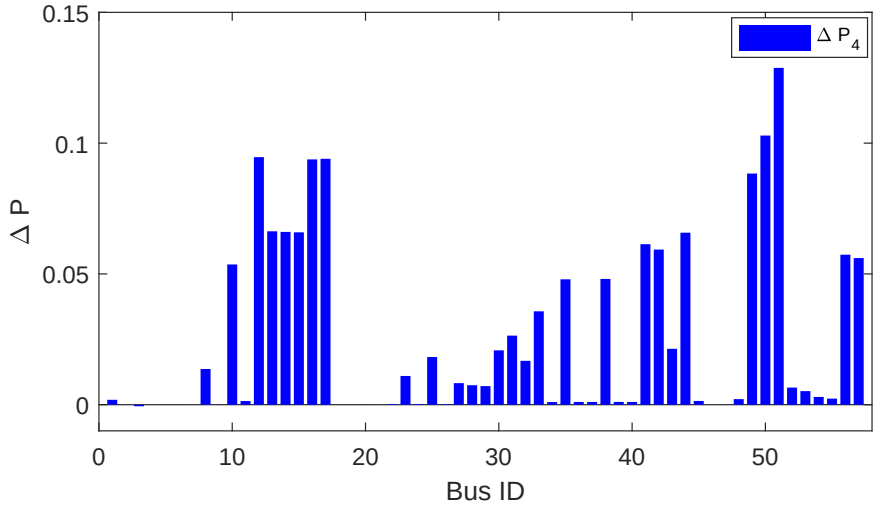

Figure 5: Distribution of changes of injected power on each bus using NPS.

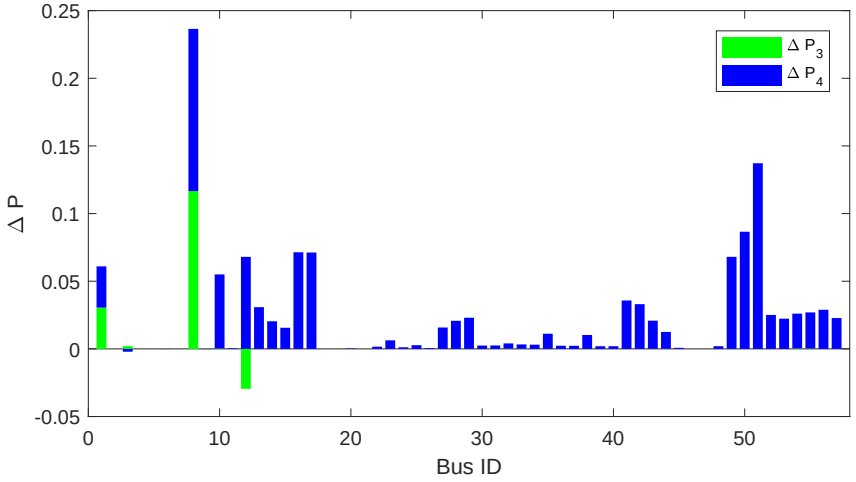

Figure 6: Distribution of changes of injected power on each bus using RPS.

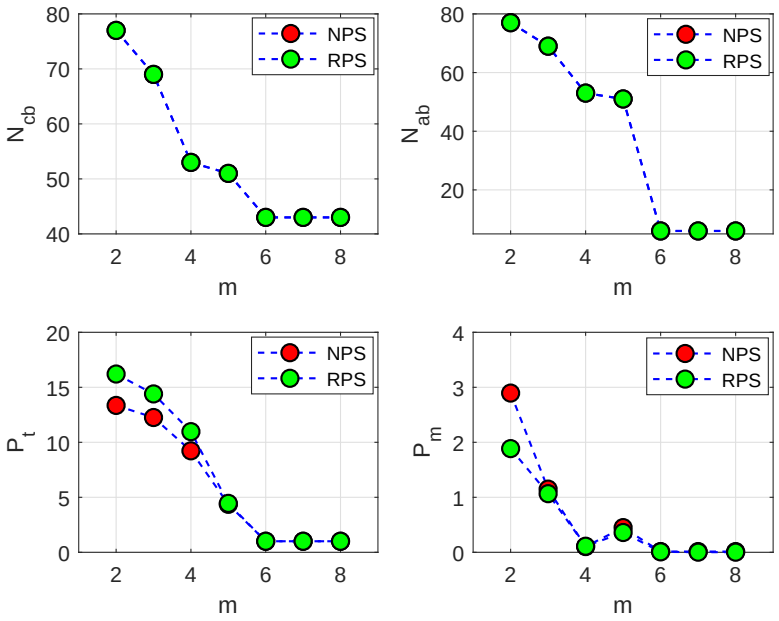

Figure 7: Comparison between NPS and RPS with different prediction horizons m on IEEE 57 Bus System. N_{cb} and N_{ab} refer to the number of connected branches and the number of active branches with power flow at the end of cascading failures, respectively. P_t and P_m represent the total power flow and the total amount of changes of injected power on buses, respectively.

$m \geq 6$. This is because the cascading failure process comes to an end at $m = 6$ and there is no chance that protection schemes can prevent power grids from blackouts.

5.3 The Effect of Parameter W

The parameter W describes the bus weight in the optimal adjustment of injected power on buses. To be specific, the buses with larger weights are deemed less significant in power networks, thus WAPCS prefers to adjust the injected power on these buses during emergency. This section aims to investigate the effects of W on the performance of protection schemes. For simplicity, we assign the same weight W_l to load buses and the same weight W_g to generator buses and take into account the weight distribution and proportion $\gamma = W_g/W_l$ on the two types of buses. Numerical simulations are conducted to implement NPS and RPS on the IEEE 57 Bus Systems with the same initial disturbance, respectively (*i.e.*, tripping Branch 10). For NPS, the protective action is implemented at the 4th cascading step, while remedial actions are taken at the 3rd and 4th cascading steps for RPS. Then we look into the power transmission and intact branches in the final cascading step by tuning the parameter γ from 0.1 to 10 gradually. Figure

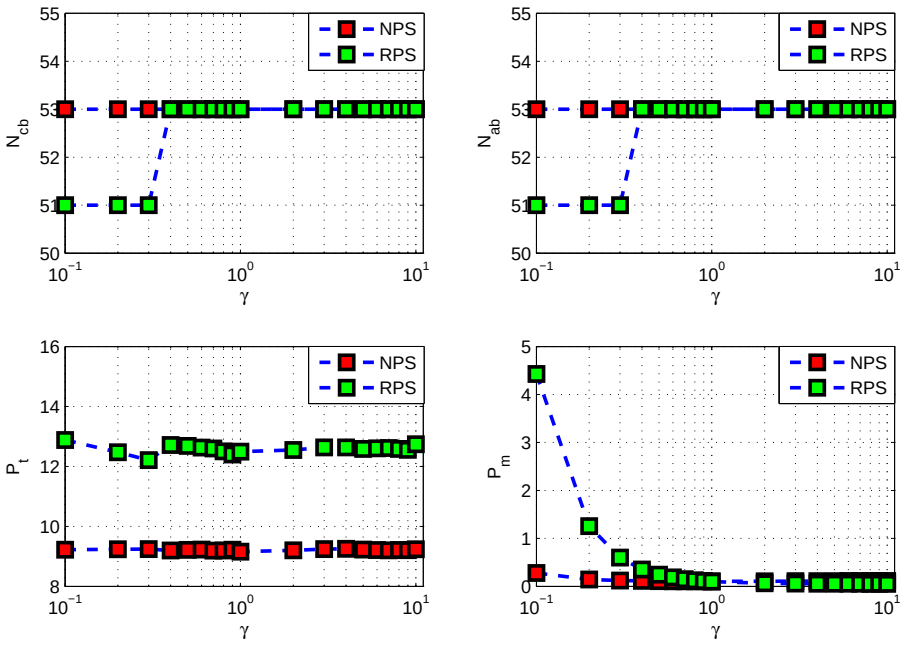

Figure 8: The effect of weight proportion γ on the final configuration of power systems. N_{cb} and N_{ab} refer to the number of connected branches and the number of active branches with power flow at the end of cascading failures, respectively. P_t and P_m represent the total power flow and the total amount of changes of injected power on buses, respectively.

8 presents the dependence of connected branches N_{cb}, active branches N_{ab}, the power flow P_t and the change of injected power on buses P_m on the parameter γ in the final configuration. It is observed that NPS is insensitive to the variation of γ, and all the four measures keep stable. In contrast, RPS behaves differently as γ varies in the range of $[0.1, 1]$. Specifically, N_{cb} and N_{ab} jump from 51 to 53 as γ increases from 0.3 to 0.4. In addition, P_m declines greatly as γ varies from 0.1 to 0.3. It is worth pointing out that RPS outperforms NPS in terms of total power transmission after terminating the cascading outages. Compared with NPS, RPS ensures the more power flow with the fewer changes of injected power on buses when γ is larger than 1. In both NPS and RPS, we can observe that N_{cb} is always equal to N_{ab} for the same parameter γ.

5.4 Other Test Systems

Two protection schemes are also implemented on IEEE 118 Bus System and IEEE 300 Bus System to validate the proposed approach. Specifically, Branch 3 is tripped as the initial disturbance to trigger the cascading failure of 118-bus system. NPS is implemented at 6th cascading step to protect power grids against blackouts, and RPS is taken at the 5th and 6th cascading steps. Both NPS and RPS achieve the same performance in terms of N_{cb} and N_{ab} (i.e., $N_{cb} = 59$ and $N_{ab} = 58$ for both NPS and RPS). RPS outperforms NPS in terms of the total power flow on branches because of $P_t = 20.4$ for RPS and $P_t = 18.4$ for NPS. In addition, it follows from $P_m = 0.06$ for RPS and $P_m = 0.29$ for NPS that RPS can protect power grids against blackouts with a lower cost (i.e., the fewer changes of injected power on buses) in comparison to NPS. Figures 9 and 10 present the changes of injected power on each bus of the IEEE 118 Bus System by taking NPS and RPS, respectively. As we can see in Fig. 9, the largest change of injected power occurs on Bus 59 with NPS. Since most changes of injected power are positive, the protection action of load shedding is taken on most buses. Similarly, the largest change of injected power also occurs on Bus 59 with RPS in Fig. 10. In terms of changes of the injected power on buses, it is suggested that more efforts are taken to prevent the cascades at the 6th cascading step.

As for the 300-bus system, Branch 6 is tripped as the initial disturbance to start cascading failures of power grids. NPS is implemented at the 4th cascading step, and RPS is taken at the 3rd and the 4th cascading steps. Compared to RPS, NPS results in more connected branches and active branches (i.e., $N_{cb} = 124$ and $N_{ab} = 66$ for NPS, $N_{cb} = 116$ and $N_{ab} = 46$ for RPS) after protective actions. In addition, NPS outperforms RPS in terms of total power flow on branches due to $P_t = 13.6$ for NPS and $P_t = 8.8$ for RPS. Nevertheless, RPS can protect power grids against blackouts with much fewer changes of injected power on buses compared to NPS (i.e., $P_m = 0.87$ for RPS and $P_m = 48.97$ for NPS), which is consistent with the conclusion in Proposition 4.1. Figures 11 and 12 show the distribution of changes of injected

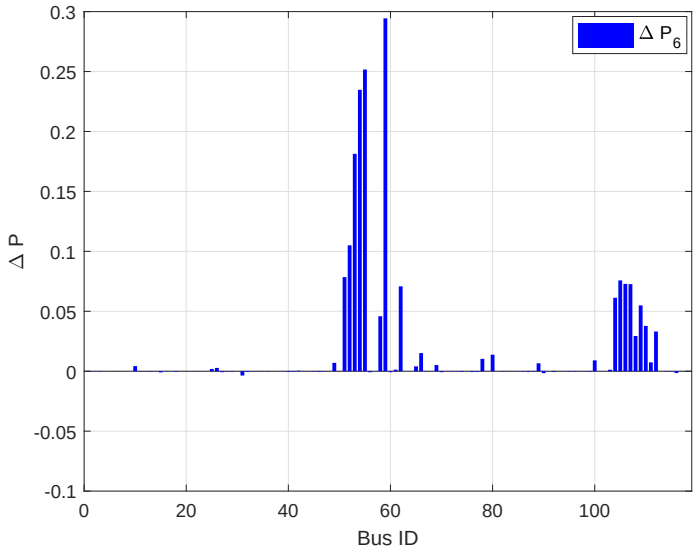

Figure 9: Distribution of changes of injected power on buses of IEEE 118 Bus System with NPS.

power on buses of the IEEE 300 Bus System by taking NPS and RPS, respectively. As we can observe in Fig. 11, Bus 171 adjusts the largest amount of injected power with NPS. In comparison, few changes of injected power are made on the buses from Bus 250 to Bus 300. In Fig. 12, it is demonstrated that both load shedding and generation ramping/tripping are taken at the 3rd and the 4th cascading steps with RPS. In terms of changes of the injected power on buses, the amount of changes at the 3rd step is comparable to that at the 4th step on the whole.

On the whole, NPS is superior to RPS in terms of computation complexity, and it takes less time for NPS to work out Optimization Problem (4) according to Saddle Point Dynamics (6). This enables NPS to efficiently implement protective actions at the early stage of cascading blackouts. Considering that more control variables in RPS are available, RPS is able to provide more flexible solutions of adjusting injected power on buses to control and protect power systems against cascading outages. In addition, RPS is able to prevent cascading outages of power grids with the fewer changes of injected power on buses.

6 Discussions

The proposed protection architecture has the potential to be extended to deal with the uncertainty of power systems and coordinate different types of protection measures for more reliable protection.

In practice, the initial contingency triggers chain reactions, which may evolve into multiple cascading

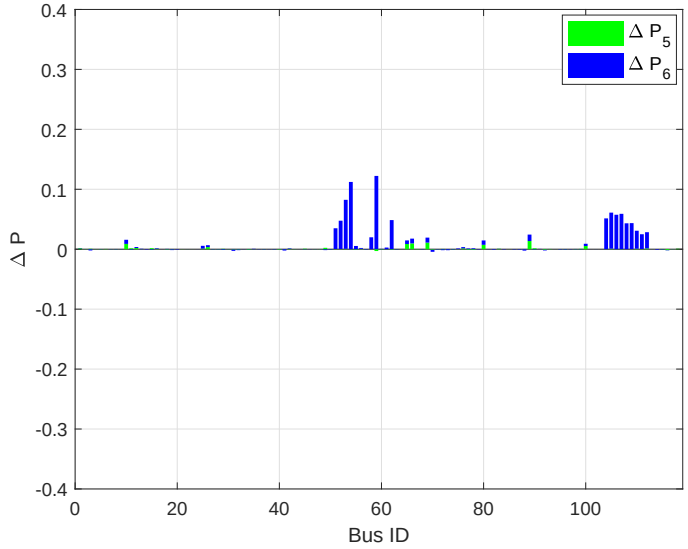

Figure 10: Distribution of changes of injected power on buses of IEEE 118 Bus System with RPS.

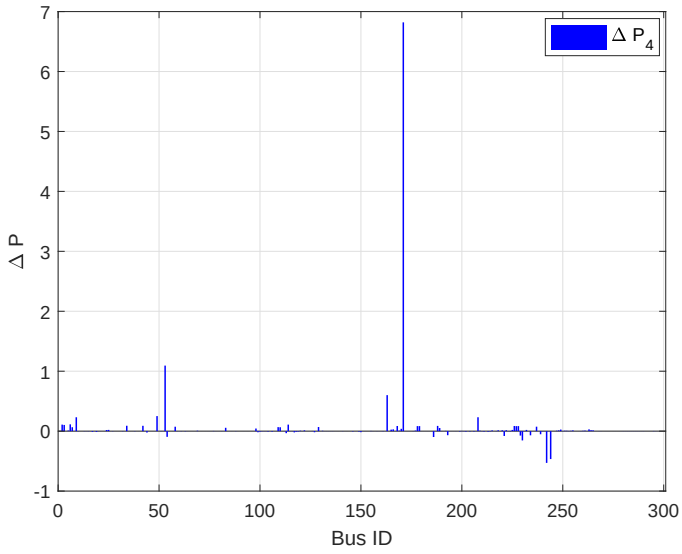

Figure 11: Distribution of changes of injected power on buses of IEEE 300 Bus System with NPS

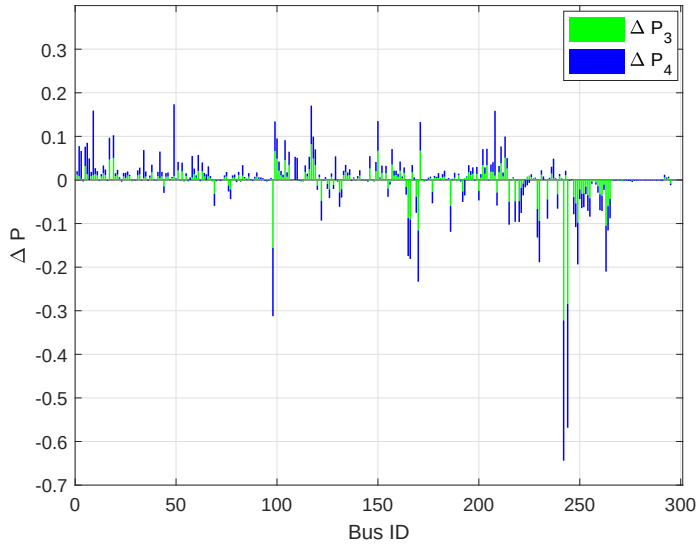

Figure 12: Distribution of changes of injected power on buses of IEEE 300 Bus System with RPS

outage paths due to various uncertainties (e.g., load variation, temperature variation, breaker faults and other unexpected events) in the period of steady-state progression. The proposed protection architecture is able to prevent the cascading failure for each specific cascading failure path. By taking into account the uncertainties in the protection architecture, multiple possible cascading failure paths and the remedial scheme for each specific path can be generated and recorded in advance. During the emergency, the power system can implement the prerecorded remedial action for the path that matches the real cascading outage path.

In case of emergency, the proposed protection architecture goes through three sequential stages: real-time detection and identification of disruptive contingencies, prediction of cascading outage paths and protection schemes based on optimal adjustment of injected power on buses. Essentially, this architecture is also compatible to other protection measures such as proactive line tripping, the online adjustment of FACTS devices and the isolation of faulted elements. More effective protection of power grids can be achieved with the coordination of different types of protection schemes. Specifically, multiple possible cascading failure paths can be described as the corresponding trajectories in the state space, and the objective is to terminate the evolution of each state trajectory by cooperatively implementing multiple protection schemes with the least cost (which may have different definitions e.g., power loss, network connectivity, fluctuation of voltage and frequency, etc., in different applications).

7 Conclusions

In this paper, we aim to propose a model predictive approach for the real-time protection of power grids against blackouts. A protection architecture was adopted to identify the initial contingency, predict the cascading failure paths and compute the optimal protection strategies. The proposed protection architecture overcomes the shortcoming of the classic SPSs and opens up the opportunity to develop the disturbance related protection schemes. Based on the protection architecture, two types of protection schemes (i.e., NPS and RPS) were designed to prevent the cascading outage of power systems. The first scheme NPS takes remedial actions at a given cascading step, while the second one implements the corrective control at two consecutive cascading steps. Moreover, It is proved that RPS does not underperform NPS in terms of minimizing the changes of injected power on buses, and these two schemes are able to achieve the optimal adjustment of injected power on buses against blackouts. Finally, extensive simulations were conducted to validate the proposed approach and theoretical results. It is demonstrated that the protection schemes perform well on different IEEE test systems. Regarding our future research work, other than the possible extensions as mentioned in Section 6, we may also study on distributed protection scheme, where challenging issues such as synchronization, convergence rate and fault tolerance will be carefully investigated.

Acknowledgment

The authors wish to thank the anonymous reviewers for their constructive comments and valuable suggestions. This work is partially supported by the Future Resilient Systems Project at the Singapore-ETH Centre (SEC), which is funded by the National Research Foundation of Singapore (NRF) under its Campus for Research Excellence and Technological Enterprise (CREATE) program. It is also partially supported by Ministry of Education of Singapore under contract MOE2016-T2-1-119.

8 Appendix

This section presents the mathematical definition of the operators $*$ and -1^* and the proofs of Equation (2) and Proposition 3.3 in details.

8.1 Definition of the Operators $*$ and -1^*

Suppose the nodal admittance matrix $Y_b^k = A^T \,\mathtt{diag}(Y_p^k)A$ is composed of q isolated subnetworks denoted by $\mathrm{S}_i, i \in I_q = \{1,2,...,q\}$ and each subnetwork S_i includes k_i buses. Let $V_i = \{i_1, i_2, ..., i_{k_i}\}$ denote the set of bus IDs in the subnetwork S_i, where i_1, i_2,..., i_{k_i} denote the bus IDs. Notice that Bus i_1 in Subnetwork S_i is designated as the reference bus. Moreover, the nodal admittance matrix of the i-th subnetwork can be computed as $Y_{b,i}^k = \mathscr{E}_i^T Y_b^k \mathscr{E}_i$, $i \in I_q$, where $\mathscr{E}_i = (e_{i_1}, e_{i_2}, ..., e_{i_{k_i}})$. Then the operators $*$ and -1^* are defined as follows [26].

Definition 8.1. *Given the nodal admittance matrix Y_b^k, the operators $*$ and -1^* are defined by*

$$\left(Y_b^k\right)^* = \sum_{i=1}^{q} \mathscr{E}_i \left(\begin{array}{c|c} 0 & 0_{k_i-1}^T \\ \hline 0_{k_i-1} & I_{k_i-1} \end{array}\right) Y_{b,i}^k \left(\begin{array}{c|c} 0 & 0_{k_i-1}^T \\ \hline 0_{k_i-1} & I_{k_i-1} \end{array}\right) \mathscr{E}_i^T$$

and

$$\left(Y_b^k\right)^{-1^*} = \sum_{i=1}^{q} \mathscr{E}_i \begin{pmatrix} 0_{k_i-1}^T \\ I_{k_i-1} \end{pmatrix} \left(\mathscr{Y}_{b,i}^k\right)^{-1} \begin{pmatrix} 0_{k_i-1} & I_{k_i-1} \end{pmatrix} \mathscr{E}_i^T,$$

respectively, where

$$\mathscr{Y}_{b,i}^k = \begin{pmatrix} 0_{k_i-1} & I_{k_i-1} \end{pmatrix} Y_{b,i}^k \begin{pmatrix} 0_{k_i-1}^T \\ I_{k_i-1} \end{pmatrix}.$$

I_{k_i-1} is the $(k_i-1)\times(k_i-1)$ identity matrix, and 0_{k_i-1} denotes the (k_i-1) dimensional column vector with zero elements.

8.2 Proof of Equation (2)

According to the DC power flow equation, we have $\theta^k = (B^k)^{-1^*}P$, where $B^k = A^T diag(Y_p^k)A$ and $\theta^k = (\theta_1^k, \theta_2^k, ..., \theta_{n_b}^k)^T$. Let B_{ij}^k denote the element in the i-th row and j-th column of the matrix B^k. Then the power flow from Bus i to Bus j can be computed by

$$\begin{aligned} P_{ij}^k &= B_{ij}^k(\theta_i^k - \theta_j^k) \\ &= e_i^T B^k e_j (e_i - e_j)^T \theta^k \\ &= e_i^T B^k e_j (e_i - e_j)^T (B^k)^{-1^*} P \\ &= e_i^T A^T diag(Y_p^k) A e_j (e_i - e_j)^T (A^T diag(Y_p^k)A)^{-1^*} P. \end{aligned}$$

8.3 Proof of Proposition 3.3

Design Lyapunov function as follows

$$V(P,\lambda,\tau)=\frac{1}{2}(\|P-P^*\|^2+\|\lambda-\lambda^*\|^2+\|\tau-\tau^*\|^2)$$

The time derivative of $V(P,\lambda,\tau)$ along Saddle Point Dynamics (6) gives

$$\dot{V}(P,\lambda,\tau)=(P^*-P)^T\nabla_P L(P,\lambda,\tau)+(\lambda-\lambda^*)^T[\nabla_\lambda L(P,\lambda,\tau)]_\lambda^+ +(\tau-\tau^*)^T[\nabla_\tau L(P,\lambda,\tau)]_\tau^+$$

Equation (7) leads to

$$(\lambda-\lambda^*)^T[\nabla_\lambda L(P,\lambda,\tau)]_\lambda^+ \le (\lambda-\lambda^*)^T\nabla_\lambda L(P,\lambda,\tau)$$

and

$$(\tau-\tau^*)^T[\nabla_\tau L(P,\lambda,\tau)]_\tau^+ \le (\tau-\tau^*)^T\nabla_\tau L(P,\lambda,\tau).$$

Since $L(P,\lambda,\tau)$ is convex in P and concave in λ and τ, we have

$$(P^*-P)^T\nabla_P L(P,\lambda,\tau)\le L(P^*,\lambda,\tau)-L(P,\lambda,\tau)$$

and

$$(\lambda-\lambda^*)^T\nabla_\lambda L(P,\lambda,\tau)+(\tau-\tau^*)^T\nabla_\tau L(P,\lambda,\tau)\le L(P,\lambda,\tau)-L(P,\lambda^*,\tau^*),$$

which leads to

$$\begin{aligned}\dot{V}(P,\lambda,\tau)&\le L(P^*,\lambda,\tau)-L(P,\lambda,\tau)+L(P,\lambda,\tau)-L(P,\lambda^*,\tau^*)\\&=[L(P^*,\lambda,\tau)-L(P^*,\lambda^*,\tau^*)]+[L(P^*,\lambda^*,\tau^*)-L(P,\lambda^*,\tau^*)]\end{aligned}$$

Moreover, it follows from $L(P^*,\lambda,\tau)-L(P^*,\lambda^*,\tau^*)\le 0$ and $L(P^*,\lambda^*,\tau^*)-L(P,\lambda^*,\tau^*)<0$ that $\dot{V}(P,\lambda,\tau)<0$. This indicates $V(P,\lambda,\tau)$ converges to 0 (and P also converges to the optimal value P^*) as time goes to infinity. The proof is thus completed.

References

[1] M. Begovic, D. Novosel, D. Karlsson, C. Henville, and G. Michel, "Wide-area protection and emergency control," *Proceedings of the IEEE*, 93(5), 876-891, 2005.

[2] Z. Bo, X. Lin, Q. Wang, H. Yi, and F. Zhou, "Development of power system protection and control," *Protection and Control of Modern Power Systems*, (2016): 1-7.

[3] L. Hewitson, B. Mark, and B. Ramesh, Practical power system protection. Elsevier, 2004.

[4] A. Molina-Cabrera, M. A. Rios, Y. Besanger, and N. HadjSaid, "A latencies tolerant model predictive control approach to damp Inter-area oscillations in delayed power systems," *International Journal of Electrical Power & Energy Systems*, 98, 199-208, 2018.

[5] I. Xyngi, and P. Marjan, "An intelligent algorithm for the protection of smart power systems," *IEEE Transactions on Smart Grid*, 4(3), 1541-1548, 2013.

[6] L. Heng, et al.,"Reliable GPS-based timing for power systems: A multi-layered multi-receiver architecture," Power and Energy Conference at Illinois (PECI), IEEE, 2014.

[7] V. Madami, M. Adamiak, and M. Thakur, "Design and implementation of wide area special protection schemes," Protective Relay Engineers, 2004 57th Annual Conference for. IEEE, 2004.

[8] M. Zima, Special protection schemes in electric power systems. Chicago, *Technical Report*, 2002.

[9] V. Centeno, A. G. Phadke, A. Edris, J. Benton, M. Gaudi, and G. Michel, "An adaptive out-of-step relay for power system protection," *IEEE Trans. Power Del.*, 12(1), 61-71, 1997.

[10] B. Milosevic and M. Begovic, "Voltage-stability protection and control using a wide-area network of phasor measurements," *IEEE Transactions on Power Systems*, 18(1), 121-127, 2003.

[11] Y. Zhu, S. Song, and D. Wang, "Multiagents-based wide area protection with best-effort adaptive strategy," *International Journal of Electrical Power & Energy Systems*, 31(2-3), 94-99, 2009.

[12] F. Aminifar, et al., "Synchrophasor measurement technology in power systems: Panorama and state-of-the-art," *IEEE Access*, 2, 1607-1628, 2014.

[13] W. Lu, et al., "Blackouts: Description, analysis and classification," *Proceedings of the 6th WSEAS International Conference on Power Systems*, Lisbon, Portugal, September 22-24, 2006.

[14] UCTE Investigation Committee, "Interim Report of the Investigation Committee on the 28 September 2003 Blackout in Italy," UCTE Report, October 27, 2003.

[15] NERC Steering Group,"Technical analysis of the August 14, 2003, blackout: What happened, why, and what did we learn," Report to the NERC Board of Trustees, 2004.

[16] J. Yan, Y. Tang, H. He, and Y. Sun, "Cascading failure analysis with DC power flow model and transient stability analysis," *IEEE Transactions on Power Systems*, 30(1), 285-297, 2015.

[17] O. A. Mousavi, M. J. Sanjari, G. B. Gharehpetian, R. A. Naghizadeh, "A simple and unified method to model HVDC links and FACTS devices in DC load flow," *Simulation*, 85(2), 101-109, 2009.

[18] A. G. Phadke, and J. S. Thorp, "History and applications of phasor measurements," In Power Systems Conference and Exposition, PSCE'06. 2006 IEEE PES (pp. 331-335).

[19] V. Terzija, G. Valverde, D. Cai, P. Regulski, V. Madani, J. Fitch, and A. Phadke, "Wide-area monitoring, protection, and control of future electric power networks," *Proceedings of the IEEE*, 99(1), 80-93, 2011.

[20] A. Omid, Y. Yuan, R. Dobbe, A. Meier, S. Low, and C. Tomlin, "Event detection and localization in distribution grids with phasor measurement units," arXiv preprint at https://arxiv.org/abs/1611.04653.

[21] A. Armenia, and J. H. Chow, "A flexible phasor data concentrator design leveraging existing software technologies," *IEEE Transactions on Smart Grid*, 1(1), 73-81, 2010.

[22] B. Naduvathuparambil, M. C. Valenti, and A. Feliachi, "Communication delays in wide area measurement systems," *Proceedings of the IEEE 34th Southeastern Symposium on System Theory*, pp. 118-122, 2002.

[23] R. Leelaruji, and L. Vanfretti, "Power System Protective Relaying: basic concepts, industrial-grade devices, and communication mechanisms," Technical Report, KTH, 2011.

[24] J. Song, et al., "Dynamic modeling of cascading failure in power systems," *IEEE Transactions on Power Systems*, 31(3), 2085-2095, 2016.

[25] G. W. Stagg, and A. H. El-Abiad. Computer Methods in Power System Analysis. McGraw-Hill, 1968.

[26] C. Zhai, H. Zhang, G. Xiao and T. Pan, "Modeling and identification of worst cast cascading failures in power systems," arXiv preprint at https://arxiv.org/abs/1703.05232.

[27] A. P. Ruszczynski, *Nonlinear Optimization*, Princeton University Press, Princeton, NJ, 2006.

[28] L. Bai, et al., "Distributed control for economic dispatch via saddle point dynamics and consensus algorithms," *Proceedings of the IEEE 55th Conference on Decision and Control*, pp. 6934-6939, 2016.

[29] A. Nedić, and A. Ozdaglar,"Subgradient methods for saddle-point problems," *Journal of Optimization Theory and Applications*, 142(1), 205-228, 2009.

[30] C. Ashish, B. Gharesifard, and J. Cortes, "Saddle-point dynamics: conditions for asymptotic stability of saddle points," *SIAM Journal on Control and Optimization* 55(1), 486-511, 2017.